Raman Resonance Effect in a Monolayer of Polypyridyl Ruthenium(II) Complex Adsorbed on Nanocrystalline TiO_2 via Phosphonated Terpyridyl Ligands

Anne Hugot-Le Goff,*,† Suzanne Joiret,† and Polycarpos Falaras‡

UPR 15 du CNRS "Physique des Liquides et Electrochimie", Université Pierre et Marie Curie, 4 Place Jussieu, 75252 Paris, Cedex 05, France, and Institute of Physical Chemistry, NCSR Demokritos, 153 10 Aghia Paraskevi Attikis, Athens, Greece

Received: March 22, 1999; In Final Form: July 14, 1999

A high Raman intensity is observed when a dye containing Ru(II) and different polypyridinium ligands is adsorbed on nanocrystalline TiO_2. This effect is attributed to a strong resonance obtained when the laser wavelength corresponds to a charge transfer between the central ruthenium atom and one of the ligands. With a judicious choice of the ligands, such modified titanium oxide electrodes used in photoelectrochemical cells can give high photocurrent efficiencies. The dye studied here contains two different ligands: L = (4,4′-Me_2-2,2′-bpy), bpy = bipyridine, and L′ = (4′-PO_3H-terpy), terpy = 2,2′:6,2"-terpyridine; in this case, the strong adsorption on TiO_2 is ensured by the PO_3H group of the L′ ligand; with the green laser line, the resonance arises also in this L′ ligand. An enhancement of the bridging ligand Raman features—not very strong but however significant—is observed during the polarization in the photoelectrochemical medium. In the case of a complicated charge-transfer complex, one can therefore identify the nature of the bridging ligand as well as, on the opposite side, assign the spectral features to a particular ligand. Very promising perspectives for the understanding of the adsorption mechanisms and of the configuration of the surface complex formed by the dye and the semiconductor during the modification of TiO_2 are now opened.

Introduction

The high Raman intensity[1] observed in Ru(II)−bipyridinium (Ru−bpy) complexes adsorbed on nanocrystalline TiO_2 (anatase), used in the dye-sensitized solar cells,[2] was attributed to a Raman resonance (RR) effect, because these dyes present a very high optical absorption in the visible range. In fact, the sensitization mechanism involves an electron injection into the semiconductor conduction band, following a metal-to-ligand charge transfer (MLCT) photoexcitation. Raman spectroscopy (RS) was extensively used to characterize this MLCT state, allowing us in particular to show that the injected electron is localized on one of the ligands.[3−6]

For efficient photosensitization, a strong (chemical) adsorption of the dye on the anatase substrate is necessary. It was obtained in particular through the carboxylation of the pyridine rings: in the case of TiO_2 photosensitization by Ru−dcbpy complexes, it has been demonstrated that intimate electronic coupling between the oxide surface and the dye is achieved by the formation of ester-like linkages.[7−8] The other ligands which are selected, such as thiocyanate[9] or triphenylphosphine (PPh_3),[10] serve essentially to enhance the optical absorption, shifting it toward the center of optical range. Very recently, new Ru−polypyridyl complexes containing terpyridine (terpy) ligands have been proved to be very efficient for the photosensitization purpose. The use of the Ru−(4,4′-Me_2-2,2′-bpy) (4′-PO_3H-terpy) (NCN) complex as a sensitizer resulted in incident photon-to-current conversion efficiencies exceeding 70%.[11] In that case the dye adsorption is ensured by a phosphonate group of the terpy ligand, which shows much stronger adhesion of the complex on TiO_2 than the carboxylato groups of the bpy ligand. The complex shows a higher stability during the potential cyclings; it does not desorb in the presence of water and can be used in a very broad pH range. Thus, although the Raman literature about Ru−terpy is limited[12,13] by comparison with the bidentate ligand, using resonance Raman spectroscopy, the lowest-energy excited state in this mixed-ligand complex has been unambiguously assigned to the Ru → P-terpy transition.[14] Furthermore, it has been demonstrated that the dye−semiconductor interaction can also be investigated. In fact, following the dye adsorption on the TiO_2 surface, important changes on the position and intensity of the different Raman vibration bands were observed.[15] It is then clear that the strong interaction between the dye and the semiconductor considerably influences the dye band energetics. As a result, such a surface complexation can also affect the lowest-energy MLCT transition involved in the photosensitization process.

On the other hand, in photoelectrochemical cells, the modified electrodes are polarized in an electrolyte containing an electron donor, allowing the restoration of the resonant form of the complex. When the Raman analysis is performed during the polarization, the spectra are modified with the appearance or enhancement of Raman modes which are otherwise not detected; in the Ru−dcbpy dyes with NCS ligand, their intensity was found to increase with the electric field.[16] They probably originate from the excited state of the sensitizer grafted on the TiO_2 surface, and display the oxide /dye interaction and the formation of a surface complex. In the dye recently studied with a PPh_3 ligand, the band intensity passes by a maximum for a particular potential,[10] in this case it is a very strong resonance effect in the spectator ligand.

These studies are obviously facilitated by the extremely large surface area covered by these dispersed materials, which must

* Corresponding author. Fax: 33 1 44 27 40 74. E-mail: ahl@ccr.jussieu.fr.
† Université Pierre et Marie Curie.
‡ Institute of Physical Chemistry, NCSR Demokritos.

10.1021/jp990975+ CCC: $18.00
Published on Web 10/07/1999

be also taken into account to explain the enhancement intensity. In this work, the interaction between the phosphonated terpyridine−Ru(II) complex and the titanium oxide was studied in detail by in situ resonance Raman spectroscopy (RRS), to elucidate the nature of the ligand−surface bond and to learn if some direct connection exists between the enhancement mechanism and the overall efficiency of the sensitized TiO_2 solar cells.

Experimental Section

Preparation of the Samples. The preparation of nanocrystalline TiO_2 samples was described elsewhere.[2,9] With this preparation, the surface can be significantly increased in a ratio $\approx$ 1000. The Ru complex is Ru−LL′(NCS) with L = (4,4′-Me_2-2,2′-bpy), L′ = (4′-PO_3H-terpy).[11] The dye adsorption was experimentally performed by immersing the TiO_2 electrodes for 1 h in a 10^{-4} M solution of the complex in ethanol, drying, and rinsing carefully with the solvent for a long enough period to eliminate all dye in excess of the first layer grafted to the surface. It was demonstrated by M. Grätzel and co-workers that this preparation leads to the grafting of one monolayer and only one.

In dye-sensitized solar cells, the photocurrent action spectrum generally matches well the dye absorption spectrum. Thus, in the case of the Ru−terpy complex, it has been observed that the photocurrent action spectrum of the modified anatase samples pass by a maximum ($\approx$70%) for a wavelength of 510 nm, where the complex presents a broad and very intense MLCT absorption band (μ = 8500 dm^3 mol^{-1} cm^{-1}).[14]

Electrochemistry. The modified samples were polarized in acetate buffer (pH = 4.5), with 0.01, 0.1, or 1M KI, or even without electron donor, between −400 and +400 mV/SCE.

Raman Analysis. The Raman spectrometer is a DILOR OMARS 89 equipped with a microscope and a multichannel detection. The total time to record one spectrum is generally about 200 s. Owing to the microscope, the absence of degradation at the laser impact point is verified after the experiments. During the Raman analysis, the cell current was recorded and presented sharp and strong increases (photocurrents) followed by decays, in phase with the light pulses. The 514.5 nm argon line, very near that of the resonance condition is used with a power of 1−5 mW. Spectra acquisition was attempted using a He−Ne red laser; it is checked that it is impossible to obtain any spectrum, using this excitation, which rules out the intervention of a SERS effect added to the RR effect.

Results

The Raman spectra of the sensitized TiO_2 electrodes have been measured (ex situ and in situ) by using 514.5 nm excitation, which is near the MLCT absorption maximum (498 nm, ϵ = 8500 M^{-1} cm^{-1}) of the complex. The high and lower wavenumber parts of spectra obtained during the polarization of the modified electrode in a solution containing 0.1 M KI are given in Figure 1 for three potentials: −400, 0, and +400 mV; the spectral features (bands shapes and relative intensities) are independent of the polarization potential. However, because of the necessary spectra treatment (smoothing and background suppressing) the position of the smaller bands can shift and the figures are labeled to show the uncertainty range. Despite a weak intensity increase in the anodic range, no direct connection with the photoeffect is obvious; however, there is a strong variation of the Raman intensity with the electron donor concentration in the electrolyte, and spectra obtained at V = +200 mV in the presence of high and low KI molarities are given (together with the ex situ spectrum) in Figure 2. The spectral features do not depend on the electron donor concentration, but the spectra are drawn with different Y-scales because of their intensity increase of more than 1 order of magnitude passing from KI = 0.01 M to KI = 1 M. The ratio of several band intensities to the ex situ intensity is given in Figure 3. Contrarily to the case of the Ru−bpy dyes studied in ref 16, it was even possible to obtain a spectrum without an electron donor, which shows the improvement of the grafted complex stability; the surface is, however, rapidly damaged if an electron donor is not added to the solution.

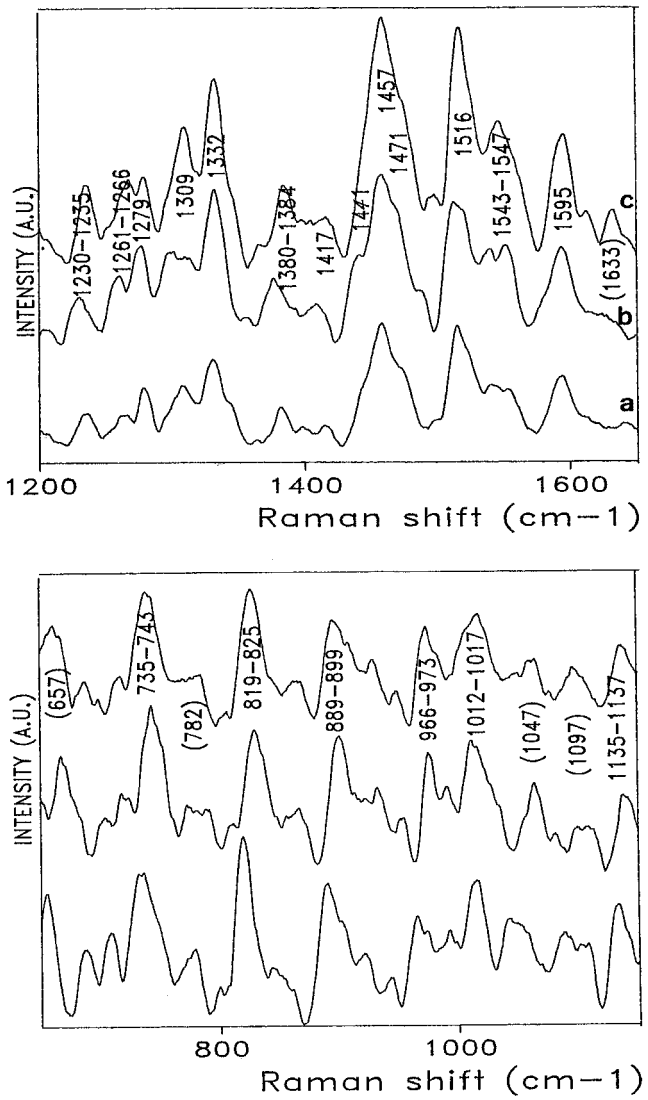

Figure 1. Raman spectra (λ = 514.5 nm) of Ru−(Me_2-bpy)(PO_3H-terpy)(NCN) adsorbed on TiO_2 during the polarization in acetate buffer + 0.1 M KI solution at (a) −400, (b) 0, (c) + 400 mV/SCE. The dispersion of experimental values is given.

In Figure 2, the ex situ dye spectrum was obtained first on the pristine surface before polarization, then verified after the polarization experiments; it can be compared to the literature available results. Several adsorbed mixed-ligand (py, bpy, terpy) complexes were studied by comparison of their experimental spectra with normal-mode calculations of the Raman band wavenumbers;[13] the spectra were obtained with the 514.5 nm argon laser line after adsorption on silver colloids, which means that the enhancement is due partly to SERS (surface-enhanced Raman effect), and not just to RR, such as in the case of the present paper, that brings a noticeable shift of the wavenumbers. One of these complexes containing at the same time terpy

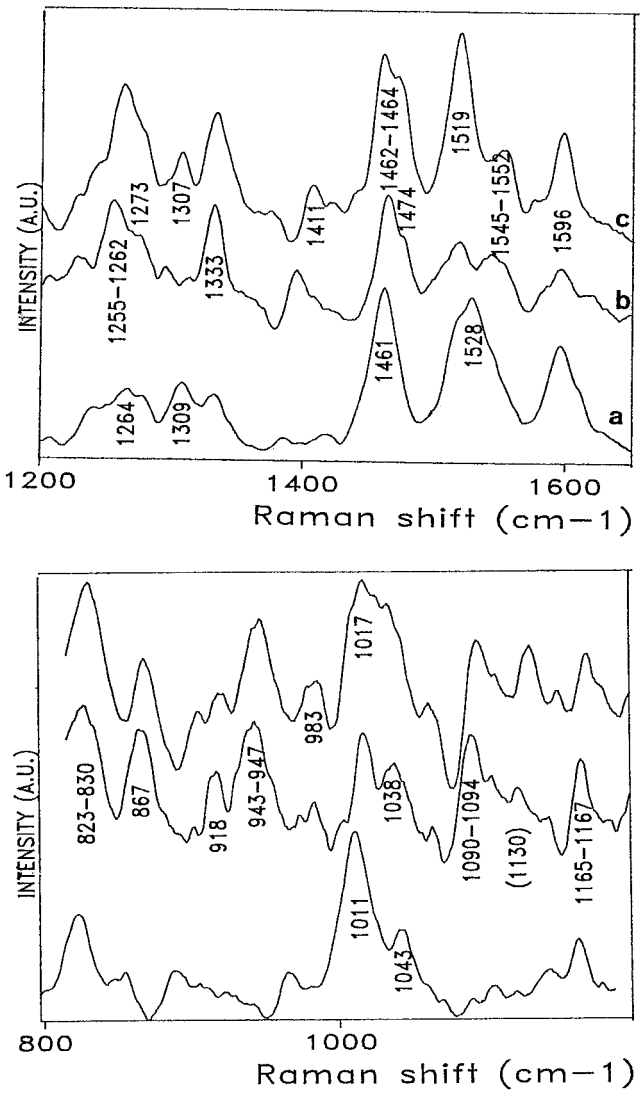

Figure 2. Raman spectra (λ = 514.5 nm) of Ru−(Me_2-bpy)(PO_3H-terpy)(NCN) adsorbed on TiO_2 during the polarization at 200 mV/SCE in acetate buffer + (b) 0.01 M KI, (c) 1 M KI. Lower plot (a): ex situ spectrum of the unpolarized sample. The dispersion of experimental values is given.

(nonsubstituted by the phosphonate group) and Me_2-bpy ligands can be compared to Ru−LL′(NCS), the difference coming from the adsorption through phosphonate. Elsewhere, M. Grätzel and co-workers published recently[14] the ex situ Raman spectrum of Ru−LL′(NCS) in solution; a difference is again expected between the spectra of a dye either adsorbed or in solution. The Raman peak values are reported in Table 1 together with the literature results,[13,14] including the terpy and bpy ligands, the theoretical values obtained by normal-mode computations program and the mode assignments assumed in refs 12 and 13. The band intensity (weak, mean, strong) is indicated. All these values were obtained with the green 514.5 nm laser line; however, in ref 14, spectra obtained with green (resonance mainly in terpy) and blue (resonance mainly in bpy) excitations have been compared, which allows us to assign a peak to a specific ligand: therefore in the first column, the frequencies tentatively correlated to terpy are in bold characters, while those correlated to bpy are underlined.

It is well established that the (C_{2v}) 21-atom Ru−bpy unit possesses 20 Raman active A_1 modes,[17] four of which are C−H stretches occurring above 2500 cm^{-1} (and are not concerned with this work). The five ν(C−C) and two ν(C−N) stretching

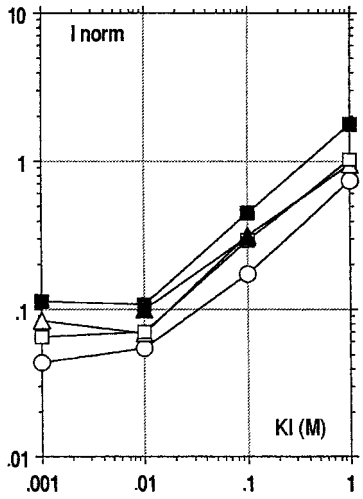

Figure 3. Intensity of some Raman bands (normalized by the ex situ intensity) in function of the KI molarity: ○ 1593 cm^{-1}, △ 1540 cm^{-1}; □ 1457 cm^{-1}, ▲ 1380 cm^{-1}, ■ 1277 cm^{-1}.

coordinates may couple with four in-plane δ(CCH) hydrogen wagging coordinates to give rise to eleven modes between ~1650 and 1000 cm^{-1}. These are labeled ν_5 through ν_{15} in Table 1. The Ru−bpy unit possess also five lower frequency modes which are labeled $\nu_{16} - \nu_{20}$. The (C_{2v}) 30-atom Ru-tpy possesses 28 Raman active modes (ω). The joined analysis of the results given in refs 12−14 allows us in principle to discriminate if a mode originates from the bpy or terpy ligand. However, some assignments appeared questionable, when the difference between calculated and experimental values reachs several tens cm^{-1}. In fact, taking into account the proximity of the similar modes wavenumbers in bpy and terpy elements (ν_5 and ω_7, ν_6 and ω_9, ν_7 and ω_{10}, ν_9 and ω_{13}, ν_{10} and ω_{14}), the assignment is far from simple, in particular for the ring skeletal stretchings. In the C−H bending range, one can see also the proximity of bpy and terpy vibrations.

The ex situ spectrum of the adsorbed dye presents three strong ring skeletal stretchings at 1595, 1528, and 1461 cm^{-1}. The second of these bands is especially interesting: it corresponds to the sum of three modes, ω_8, ν_6, and ω_9. This band is not split in the ex situ spectrum (neither in the SERS experiments[13]); the separation was better in solution, in particular with the green excitation.[14] Under polarization the three bands are separated, which means that the vibrations of bpy or terpy rings which were mixed in the ex situ spectrum are now individualized, and in particular ω_8, which originates from the center pyrydine ring. For the third peak, the same phenomenon is observed with the detection of ν_7 and ω_{11} not detected ex situ.

In the spectral range below, the influence of C−H bending begins to appear. Weak ex situ peaks at 1418 and 1384 cm^{-1} are followed by a broad band formed by five medium peaks at 1334, 1307, 1277, 1264, and 1239 cm^{-1}, a weak peak at 1165 cm^{-1}, and a medium band with a peak at 1011 cm^{-1}. A striking phenomenon is that the enhancement of this whole range under polarization, making visible all the theoretically expected spectral lines (even weak) which were not well separated in the ex situ spectrum, in particular in the 1200−1300 cm^{-1} range with the large contribution of C−H bendings. Under polarization, the phosphonate anions internal stretching modes in the range 850−1150 cm^{-1} which hardly emerge from the background in the ex situ spectrum can also be detected. Metallic phosphates can present bands at, at least, 1060, 990, 940, 890 cm^{-1}, depending on the cation and hydration;[18] here the bands around 890, 940, and 970/980 cm^{-1} are unambiguously assigned

TABLE 1: Raman Bands (cm^{-1}) of the Phosphonate Ru−terpy Complex (1) Attached on a TiO_2 Thin-Film Surface (ex situ and under polarization) with 514.5 nm Excitation[a]

(**1**) expt. ref 14	[Ru(terpy)(Me_2bpy)]$^{2+}$ expt, ref 13	band assignments for terpy (ω) or bpy (ν) ligands refs 12, 13	terpy ligand ref 13 calcd	terpy ligand ref 13 expt	bpy ligand ref 13 calcd	bpy ligand ref 13 expt	(**1**)/TiO_2 expt ex situ (this work)	(**1**)/TiO_2 expt under pol (this work)
1619(w)		ν_5, py ring stretch.			1605	1606(s)		1628/33(w)
1601(m)	1603(m)	ω_7, outer py ring def.	1589	1602(s)			1596(s)	1595/6(m)
1560(w)	1550(s)	w_8, center py ring def.	1585	1555(s)				1543/7(m)
1548(w)		ν_6, py ring stretch.			1557	1562(s)		
1520(s)		ω_9, outer py ring def.	1569	1568(s)			1528(s)	1516/9(s)
		ν_7, py ring stretch.			1471	1491(s)		1471/4(w)
1472(s)	1491(s)	ω_{10}, outer py	1469	1497(s)			1461(s)	1457/64(s)
	1469(m)	ω_{11}, movement 3 py	1423	1480(m)				1441(s)
1414(w)		ν_8, py ring def.			1435	1452(w)	1418(w)	1411/7(w)
1393(w)	1387(w)	ω_{12}, center py mode	1365	1394(w)			1384(w)	1380/4(w)
		ν_9, op py ring def.			1333	1320(s)		
1339(m)	1327(m)	ω_{13}, outer py	1342	1328(s)			1334(w)	1332(s)
1320(w)		ν_{10}, py ring def.			1296	1275(m)	1309(m)	1307/9(m)
1283(w)	1284(w)	ω_{14}, outer py	1267	1270(w)			1277(w)	1277/9(w)
1269(w)								
1253(m)		ν_{11}			1224	1175(m)	1264(m)	1255/66(m)
1248(w)							1239(w)	1230/5(w)
	1186(s)	ω_{17}, center py stretch	1121	1186(w)				1193(w)
1200(w)		ν_{12}, C−H bend			1182	1112		
1164(w)	1165(m)	ω_{15}, C−H bend	1145	1169(w)			1165(m)	1165/7(w)
		ν_{13}, C−H bend			1115	1065(w)		
1137(w)	1136(w)	ω_{16}, C−H bend	1131	1115(w)			1142(m)	1135/7(w)
1059(w)		ν_{14}, C−H bend			1096	1042(s)		
	1095(w)	ω_{18}, C−H bend	1096	1098(w)			1105(w)	1097(w)
	1064(w)	ω_{18}, outer py ring def.	1073	1043(w)				
1025(w)		ν_{15}, C−H bend			1036	1027(w)	1043(m)	1038/47(w)
	1043(m)	ω_{20}, C−H bend	1061	1031(w)				
	1014(s)	ω_{21}, center py stretch	952	1009(s)			1011(s)	1012/7(w)
		phosph						966/73(w)
		phosph						943/7
		phosph						889/99(w)
(826)(w)		ω_{22}, o-p center + outer	894	906(w)			825(w)	819/30(w)
(742)(w)							782(w)	782(w)
	725(m)	ω_{23}, N displacemt (Ru−N)	678	723(m)			734(w)	734(w)
(690)(w)	677(w)	ω_{24}, N displacemt	587	675				
(655)(w)	642(w)	ω_{25}, N displacemt (Ru−N)					656(w)	657(w)
		anatase					639(w)	
(578)(w)			569	580				
		anatase					515(w)	
	545(w)	ω26	358	414				
		anatase					394(w)	
	394(w)							
	348(w)							
	313(w)	ω_{27}, vib. whole terpy	272	296				
		anatase					147(w)	
		ω_{28}	79					

[a] The uncertainty range of the in situ values is given. Literature data for Ru−terpy and Ru-bpy complexes in refs 12−14 are also reported for comparison and band assignment (s = strong, m = medium, and w = weak).

to the anion. Under polarization, the 1010 cm^{-1} spectral feature is clearly depleted with respect to these anions bands; the use in ref 14 of RR enabled us to relate this feature to the bpy ring and the response of terpy ligand is therefore preferred.

In the lowest wavenumber range, weak bands exist at 825 and 734 cm^{-1}, a very strong band at 639 cm^{-1} with a shoulder at about 656 cm^{-1}, then (not shown here) medium bands at 515 and 394 cm^{-1}, and finally a *very* strong band at 147 cm^{-1}. These four last features (639, 515, 394, and 147 cm^{-1}) correspond to the response of the anatase substrate. A very striking phenomenon due to the polarization is observed: the quenching of the anatase bands as shown in Figure 4, where the ex situ spectrum (Figure 4b) is compared to the spectrum obtained during the polarization at 200 mV in the presence of 1M KI (Figure 4a); the dye bands at 656, 734, and 782 cm^{-1} (better seen in the lower spectrum where the Y-scale was multiplied by 10) have comparable intensities, while the very strong 632 cm^{-1} anatase band has lost 1 order of magnitude.

To study thoroughly the results, we propose the following procedure: the spectra are cut in smaller units of 5/7 bands, corresponding to the different ranges: ring skeletal stretchings, phosphate internal modes... and decomposed using a SpectraCalc software. In each range the intensity is characterized by the band-covered area, normalized by the total area, which gives the percentage of each vibration, and this percentage is compared to its percentage in the ex situ spectrum. One can then quantitatively know how the band was enhanced or depleted by the sample polarization: the bands below 1 are depleted by the polarization; the bands above 1 are enhanced. Two examples are displayed in Figures 5 and 6. They are not spectacular modifications, since the enhancement factor is generally less than 3, and one can see for instance in Figure 5 how the 1012 cm^{-1} band characteristic of bpy is depleted with respect to the anion bands, and in Figure 6 also the depletions of the ν_{11} and ν_{10} with respect to ω_{14} and ω_{13}. The nature of the mode (enhanced or depleted by the polarization) does not modify the

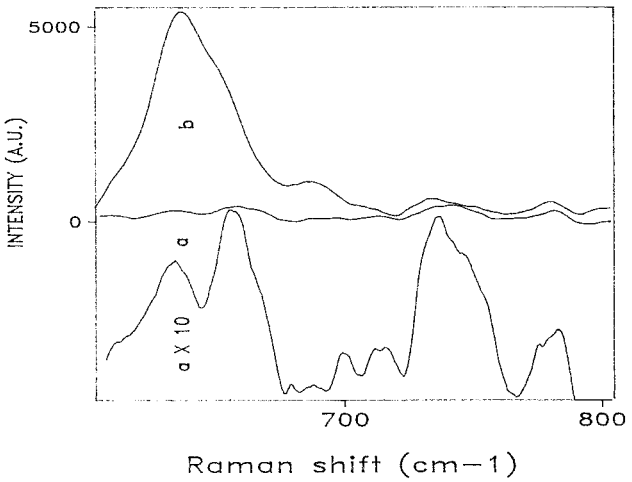

Figure 4. Raman spectra (λ = 514.5 nm) of Ru−(Me_2-bpy)(PO_3H-terpy)(NCN) adsorbed on TiO_2 (a) during the polarization in acetate buffer + 1 M KI solution at 200mV/SCE, (b) ex situ.

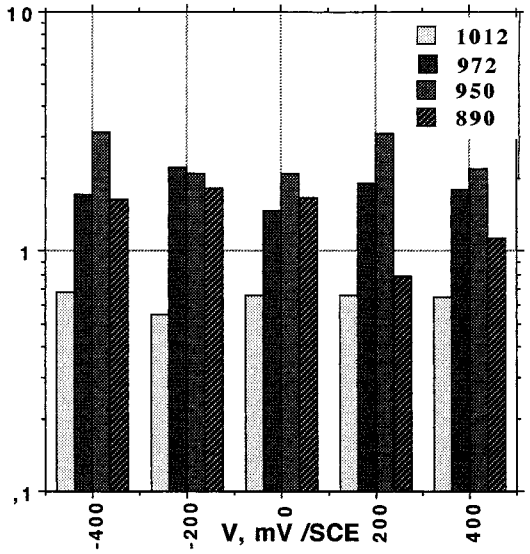

Figure 5. Ratio of the band intensities to their ex situ intensity in function of the polarization potentials in acetate buffer + 0.1 M KI solution.

relationship between the Raman intensity and the electron donor concentration, as shown in Figure 3 where the open symbols correspond to depleted modes, and the full symbols to enhanced modes.

Discussion

We saw that the global features of the ex situ spectrum given here were in correct agreement with the literature results. In the wavenumber range above 650 cm^{-1}, 17 modes ($\omega_7 - \omega_{23}$) were calculated[13] and assigned in Table 1 either to the PO_3-terpy or to the Me_2-bpy ligand. Each of these 17 modes which could not be all identified in the ex situ spectrum are now displayed, owing to polarization, when the electrode is plunged in the electrolytic cell.

The splitting of the peak at 1528 cm^{-1} (ω_9), which shifts at 1516/7 cm^{-1} while two new peaks appear in the 1543/52 cm^{-1} range is a good picture of the formation of the double Raman response. In Ru−terpy, two peaks (ω_8 and ω_9) were theoretically forecast in this range, but ω_8 is quenched in the case of mixed ligands. This vibration, which was experimentally shown in Ru−terpy but disappeared in the mixed-ligand complexes, was

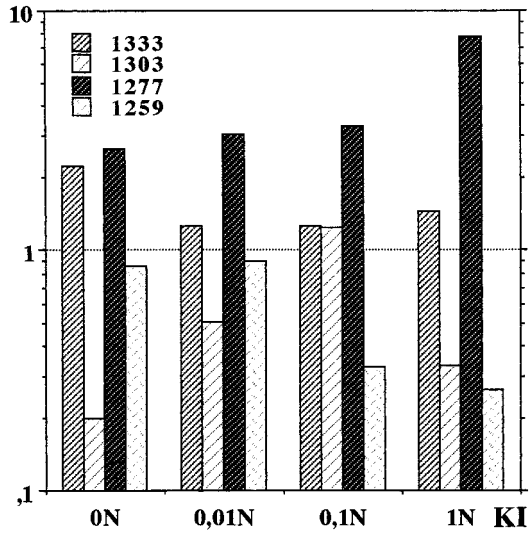

Figure 6. Ratio of the band intensities to their ex situ intensity at V = +200 mV/SCE in function of the KI concentration.

assigned to a mode in center pyridine;[13] if this assignment is correct, the mode corresponds to the complex part which is grafted to the anatase through the phosphonate group, which explains why it reappears during the polarization.

In the 1200−1400 cm^{-1} range, 5 modes (ω_{12} to ω_{16}) are foreseen. In practice, the stronger mode is ω_{13} at 1332 cm^{-1}. During the polarization, we observe an enhancement in all the range, in particular of ω_{13}, and also of ω_{12} at 1380/4 cm^{-1} and ω_{14} at 1277/9 cm^{-1}, which once more suggests a reinforcement of the PO_3-terpy ligand response. The mode at 1380 cm^{-1}, which is almost undetectable in the ex situ spectrum and reaches a noticeable intensity during the polarization is specially interesting, since it is assumed to originate in the center (or grafting) pyridine. Very small modes at ≈1230 and 1193 cm^{-1} (which was not detected in the ex situ spectrum) are enhanced enough to appear, which leads finally to the theoretical anticipation of 17 modes in the studied wavenumber range. In the 1100−1200 cm^{-1} range, the ω_{21} mode at 1011/7 cm^{-1} is on the contrary depleted by the polarization, because it originates of the M_2-bpy ligand.

The 4 bands assigned to the grafting anion in the 890−980 cm^{-1} range vary in similar ways. Changes of the anion valency with the polarization potential cannot therefore be displayed.

The spectrum of anatase substrate is almost buried under the complex spectrum; however, TiO_2 is characterized by a very high Raman cross section and in the ex situ spectrum, the ω_{24} and ω_{25} modes appear very weak in regard to the 632 cm^{-1} band of anatase. During the polarization, the surface charge of TiO_2 is so strong that the semiconducting nature of the material is lost; the interfacial layers of anatase take a metallic character, which brings the disappearance of the Raman vibrations and even introduces a screening effect of the deeper layers of TiO_2.

The changes in band intensities observed under applied bias may in general be related to nuclear displacements that distort the excited electronic state configuration from that of the ground state, these distortions becoming observable through Raman scattering under resonance conditions.[19] In fact, in the particular situation of a surface enhancement effect (SERS), two different mechanisms, electromagnetic and chemical, contribute to the overall enhancement. While the electromagnetic mechanism is a coupling with the surface plasmon resonances through the surface, microroughness and the use of very rough and fractal TiO_2 surfaces[7,20] cannot exclude such a contribution, the main

feature of the chemical mechanism is a photon-assisted charge-transfer process in the surface complex, excited by the laser radiation.[21]

The SERS effect has only been observed on certain metal surfaces, especially Ag or Au. However, very recently, SERS spectroscopy has been used to study adsorbates on semiconductor surfaces.[22] On the basis of our results a modified model analogue to that proposed for the charge-transfer process responsible for the surface-enhanced Raman scattering on complexes involving transition-metal ions and molecules having low-lying p* orbitals[21,23] can be introduced. In the same way, one cannot exclude that the photon-assisted charge-transfer process is modulated by the potential applied to the semiconductor electrode. The model we propose for the charge-transfer process responsible for the observed resonance Raman effect considers

(i) the formation of a surface complex between the dye molecule with the semiconductor oxide electrode, (ii) the existence of Ti−O−P bonds resulting from maximum overlapping and subsequent strong electronic coupling between the Ti-3d orbitals of the semiconductor conduction band and the p* orbitals of the PO_3H-terpy ligand, and (iii) the creation of a density of new states (both donor and acceptor) at the semiconductor dye interface.

The proposed modified model can explain the resonant Raman effect for the TiO_2 solar cells sensitized by the Ru−terpy complex and is in very good aggreement with the obtained results. In fact, the sensitization phenomenon involves an electron injection from the dye-excited state to the semiconductor following a rather similar process, and in both cases the Raman enhancement is achieved when the energy of the incident radiation matches that of the charge-transfer process (resonant conditions). The presence of functional groups on the ligands ensures intimate electronic contact between the dye and the semiconductor and allows efficient electron injection into the semiconductor conduction band. Earlier Raman and FTIR studies on Ru−Me_2-bpy dyes[7,24,25] have shown that the ruthenium complexes are attached to TiO_2 via an ester bond. In the case of the phosphonate Ru−terpy complex the formation of a H-bonding (P−O−H- - -O−Ti) is less probable and must be excluded, although it could lead to a relatively stable structure at the surface, because such a hydrogen bond could not facilitate the electron transport. On the contrary, the existence of a direct P−O−Ti bond is more possible and could explain the observed Raman band enhancement of the phosphonate ligand and terpyridine group as well as the concomitant strong quenching of the 632 cm^{-1} anatase band following polarization.

The important changes in the Raman bands position and intensity, especially in the 1200−1600 cm^{-1} region, are associated with the increased susceptibility of the complex to polarization induction via the phosphonate ligand, this being directly involved in the TiO_2 adsorption. It is important to note that in the potential range investigated (from +0.4 V to −0.4 V/SCE) the Raman enhancement is mainly associated with electron injection conditions. In fact, in most Ru−bpy-sensitized solar cells, even at relatively negative potentials, (i.e., −0.3 V/SCE), a photocurrent, although small, is obtained. To completely suppress electron injection, one must apply a more negative bias, lower than −0.4 V/SCE.[26] A similar behavior was also observed on TiO_2 films sensitized by the $Ru(dcbpy)_2$-(NCS) complex.[27] In that case, it is clear that suppression of the TiO_2 Raman bands deformation and decrease as well as the reappearance of the ex situ dye spectrum is observed for potentials as negative as −0.7 V/SCE. Moreover, in situ spectroelectrochemical measurements[28] have shown that the yield of electron-transfer product, Ru(III), decreases as the applied bias is switched to more negative potentials. At an applied bias of −0.7 V the only observable transient is the excited state of the complex, Ru(II)*.

In light of the above remarks it is not surprising that the degree of enhancement of the surface-binding modes is almost independent of the sign or magnitude of the applied voltage in the potential range investigated (from +0.4 V to −0.4 V/SCE). Thus, the application of a positive bias slightly favors the electron injection process into the semiconductor band gap and this helps to understand the observed weak intensity increase in the anodic range. In addition, the strong variation of the Raman intensity with the electron donor concentration in the electrolyte may result from the reaction between the oxidized form of the sensitizer and the iodide anions which regenerates the ground state of the Ru−terpy complex.

Conclusion

The modification of nanocrystalline TiO_2 surfaces by Ru−terpy complexes allows more than 1 order of magnitude of gain in the photoelectrochemical efficiency of the system. An incident photon-to-current conversion efficiency of more than 70% was observed at 510 nm.[11]

In the presence of an electric field ensuring the polarization of the organic layer, and of an electron donor in solution allowing the perpetual restoration of the dye "light absorbing" configuration, it is possible to study by Raman spectroscopy the surface complex formed by the dye and the surface titanium atoms during the adsorption, because we are in the presence of a huge enhancement effect, mainly due to Raman resonance. Although, in the two experiments, electron exchange is implied, the connection with the photoelectrochemical results is far from being simple. The delocalization of the π^* level of the pyridinium ligands and the electronic coupling between these π^* orbitals and the $Ti_{(3d)}$ ones play an important role. Thus, the electrode polarization permitted the identification of all the vibrational modes of the Ru−terpy dye in the wavenumber range above 650 cm^{-1}.

The striking result is that the role of PO_3-terpy as a bridging ligand is shown by the enhancement of all the bands originating from this ligand, with respect to the Me_2-bpy bands. The proposed modidied model for the charge transfer process not only opens promising perspectives to characterize the surface of the modified TiO_2 electrodes, but also permits answering whether the surface modification occurs via P−O−Ti or P−OH···O−Ti bonds. The model gives the possibility of better understanding the influence of the polarization on the phosphonate and terpy bands and it is consistent with the weak intensity increase in the anodic range, the strong variation of the Raman intensity with the electron donor concentration in the electrolyte, as well as the quenching of the anatase bands following polarization. A very large experimental field is opening to arrive at a full description and optimization of the photosensitization phenomenon, but it requires a significant improvement of the theoretical background.

Acknowledgment. We thank M. Grätzel's group (Lausanne, Switzerland) for donating the dye as well as the anatase substrates.

References and Notes

(1) Falaras, P.; Grätzel, M.; Hugot-Le Goff, A.; Nazeeruddin, M.; Vrachnou, E. *J. Electrochem. Soc.* **1993**, *140*, L92.

(2) Vlachopoulos, N.; Liska, P.; Augustynski, J.; Grätzel, M. *J. Am. Chem. Soc.* **1988**, *110*, 1216.

(3) Bradley, P.; Kress, N.; Hornberger, B.; Dallinger, R.; Woodruff, W. *J. Am. Chem. Soc*. **1981**, *103*, 744.
(4) Smothers, W.; Wrighton, M. *J. Am. Chem. Soc.* **1983**, *105*, 1067.
(5) Treffert-Ziemelis, S.; Golus, J.; Strommen, D.; Kincaid, J. *Inorg. Chem*. **1993**, *32*, 3890.
(6) Maruszewski, K.; Strommen, D.; Kincaid, J. *J. Am. Chem. Soc*. **1993**, *115*, 8345.
(7) Falaras, P. *Sol. Energy Mater. Sol. Cells* **1998**, *53*, 163.
(8) Duffy, N. W.; Dobson, K. D.; Gordon, K. C.; Robinson, B. H.; McQuillan, A. J. *Chem. Phys. Lett.* **1997**, *266*, 451.
(9) Nazeeruddin, M.; Kay, A.; Rodicio, I.; Humphry-Baker, R.; Müller, E.; Liska, P.; Vlachopoulos, N.; Grätzel, M. *J. Am. Chem. Soc*. **1993**, *115*, 6382.
(10) Falaras, P.; Hugot-Le Goff, A.; Bernard, M. C.; Xagas, A. To be published.
(11) Péchy, P.; Rotzinger, F.; Nazeeruddin, M.; Kohle, O.; Zakeeruddin, S.; Humphry-Baker, R.; Grätzel, M. *J. Chem. Soc. Chem. Commun*. **1995**, *1093*, 65.
(12) Hansen, P.; Jensen, P. *Spectrochim. Acta* **1994**, *50A*, 169.
(13) Schneider, S.; Brehm, G.; Prenzel, C.; Jäger, W.; Silva, M.; Burrows, H.; Formosinho, S. *J. Raman Spectrosc*. **1996**, *27*, 163.
(14) Zakeeruddin, S.; Nazeeruddin, M.; Péchy, P.; Rotzinger, F.; Humphry-Baker, R.; Kalyanasundaram, K.; Grätzel, M.; Shklover, V.; Haibach, T. *Inorg. Chem*. **1997**, *36*, 5937.
(15) Hugot-Le Goff, A.; Joiret, S.; Falaras, P.; Grätzel, M.; Péchy, P.; Vlakopoulos, N.; Zakeeruddin, M. *Proc. SPIE, SPIE Press* **1995**, *2531*, 220.
(16) Hugot-Le Goff, A.; Falaras, P. *J. Electrochem. Soc*. **1995**, *142*, L38.
(17) Danzer, G.; Kincaid, J. *J. Phys. Chem.* **1990**, *94*, 3976.
(18) Melendres, C.; Camillone, N.; Tipton, T. *Electrochim. Acta* **1989**, *34*, 281.
(19) Shi, W.; Wolfgang, S.; Strekas, T.; Gafney, H. *J. Phys. Chem.* **1985**, *89*, 974.
(20) Provata, A.; Falaras, P.; Xagas, A. *Chem. Phys. Lett.* **1998**, *297*, 484.
(21) Otto, A.; Mrozek, I.; Grabhorn, H.; Akemann, W. *J. Phys. Condens. Matter* **1992**, *4*, 1143.
(22) Quagliano, L.; Jousserand, B.; Orani D. *J. Raman Spectrosc*. **1998**, *29*, 721.
(23) Rubim, J.; Corio, P.; Ribeiro, M.; Matz, M. *J. Phys. Chem.* **1995**, *99*, 15765.
(24) Meyer, T.; Meyer, G.; Pfenning, B.; Schoonover, J.; Timpson, C.; Wall, J.; Kobusch, C.; Chen, X.; Peek, B.; Wall, C.; Ou, W.; Erikson, B.; Bignozzi, C. *Inorg. Chem.* **1994**, *33*, 3952.
(25) Murakoschi, K.; Kamo, G.; Wada, Y.; Yanagida, S.; Migazaki, H.; Matsumoto, M.; Murasawa, S. *J. Electroanal. Chem.* **1995**, *396*, 27.
(26) O'Reagan, B.; Moser, J.; Anderson, M.; Greatzel M. *J. Phys. Chem.* **1990**, *94*, 8720.
(27) Falaras, P.; Hugot-Le Goff, A.; Bernard, M. C.; Xagas A. Unpublished results.
(28) Kamat, P.; Bedja, I.; Hotchandani, S.; Patterson, L. *J. Phys. Chem.* **1996**, *100*, 4900.